

демонстрирует изменение фазового состава феррита меди после ТО при 700°C и после электрохимических экспериментов. Формирующиеся Fe-Cu композиты проявляют высокую электрокаталитическую активность в электрогидрировании органических соединений.

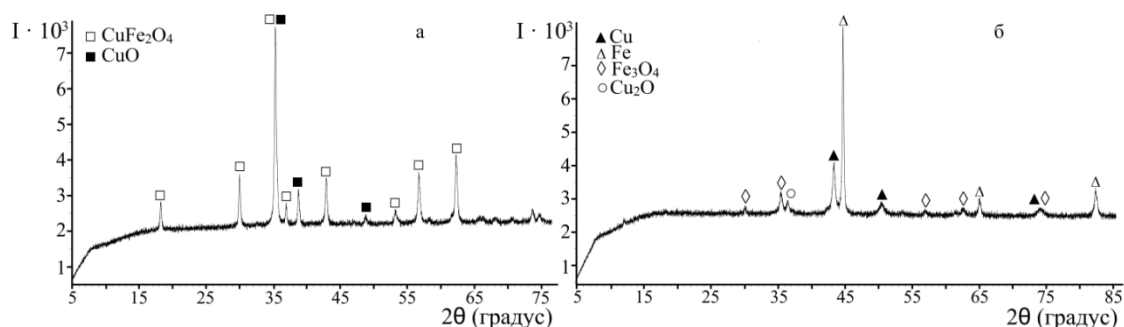


Рисунок 9 – Рентгенограммы CuFe_2O_4 после ТО при 700°C до (а) и после (б) электрохимических экспериментов

Таким образом, описанные исследования показали, что медьсодержащие композиты как без, так и с нанесением НЧ меди на полимерные и углеродные носители оказывают эффективное каталитическое действие на процессы электрохимического восстановления органических соединений и могут быть востребованы в качестве катализаторов в различных химических реакциях.

Список использованной литературы

1. Кирилос И.В. Электрокаталитическое гидрирование. – Алма-Ата: Наука КазССР, 1981. – 135 с.
2. Кирилос И.В., Мулдахметов М.З., Филимонова В.И., Бекенова У.Б. Электрокаталитическое гидрирование ацетиленовых спиртов. – Алматы: «Гылым», 1997. – 116 с.
3. Soboleva E.A., Visurkhanova Ya.A., Ivanova N.M., Beisenbekova M.E., Kenzhetaeva S.O. Ultrafine copper and nickel powders in the electrocatalytic hydrogenation of organic compounds // Хим. ж. Казахстана. – 2021. - № 2 (74). – С. 32-48.
4. Иванова Н.М., Висурханова Я.А., Соболева Е.А. Полианилин-металлические композиты. Синтез, строение и электрокаталитическая активность. – Караганда: «Гласир», 2022. – 328 с.
5. Патент РК на изобретение № 33481. Способ получения металлополимерных композитов на основе полимера и соли металла / Иванова Н.М., Соболева Е.А., Висурханова Я.А. - Бюллетень № 9 от 01.03.2019.
6. Ivanova N.M., Soboleva Ye.A., Vissurkhanova Ya.A. Synthesis of copper-carbon nanocomposites and their application as electrocatalysts // Rus. J. Appl. Chem. – 2025. – Vol. 98, № 1. – P. 10-19.
7. Muldashmetov Z.M., Ivanova N.M., Vissurkhanova Ya.A., Soboleva E.A. Preparation and electrocatalytic application of copper- and cobalt-carbon composites based on pyrolyzed polymer // Catalysts. – 2022. – Vol. 12. 862.
8. Иванова Н.М., Соболева Е.А., Висурханова Я.А., Мулдахметов З. Электрохимическое получение Fe-Cu-композитов на основе феррита меди (II) и их электрокаталитические свойства // Электрохимия. – 2020. – Т. 56, № 7. – С. 579-590.

Работа выполнена при финансовой поддержке Комитета науки МНВО Республики Казахстан (научная программа № BR24992921).

UDC 681.527.74:539.23(045)

ORGANIC ELECTROCHEMICAL RECTIFIER

Pyassov B.R., Astana IT University, Astana, Kazakhstan
Zavgorodniy A.V., Astana IT University, Astana, Kazakhstan
Akhatova Zh.Zh., Astana IT University, Astana, Kazakhstan
Dochshanov E.S., Astana IT University, Astana, Kazakhstan
Kenzhebek A., Astana IT University, Astana, Kazakhstan

In recent years, there has been a significant increase in interest in organic electrochemical transistors (OECTs) due to their unique characteristics, such as high transconductance, low operating voltage (< 1 V), and compatibility with aqueous environments. These properties make OECTs promising for applications in biosensors, bioelectronics, and neuromorphic computing systems [1-3].

A key component of OECTs, which endows them with these unique functional properties, is the organic mixed ionic-electronic conductor (OMIEC) used as the transistor channel [10]. OMIEC materials represent a class of polymers that exhibit both electronic and ionic conductivity [4].

The operating principle of OECT is based on the electrochemical doping of the OMIEC layer by ions from the solution [10]. Figure 1a shows the architecture of an OECT. In an OECT, the OMIEC-based channel is located between two electrodes - the source and the drain - and is in contact with an electrolyte on top, in which a third electrode, the gate, is immersed. The conductivity of the channel is regulated through the process of electrochemical doping.

Depending on the initial charge carrier density of the OMIEC material, OECTs are classified into devices operating in accumulation or depletion mode [5]. The main difference lies in the initial conductivity of the OMIEC layer. Let's consider the operation of an OECT in the case of a device operating in accumulation mode with a p-type OMIEC channel. Figures 1b and 1c illustrate the process of electrochemical doping of the OMIEC channel.

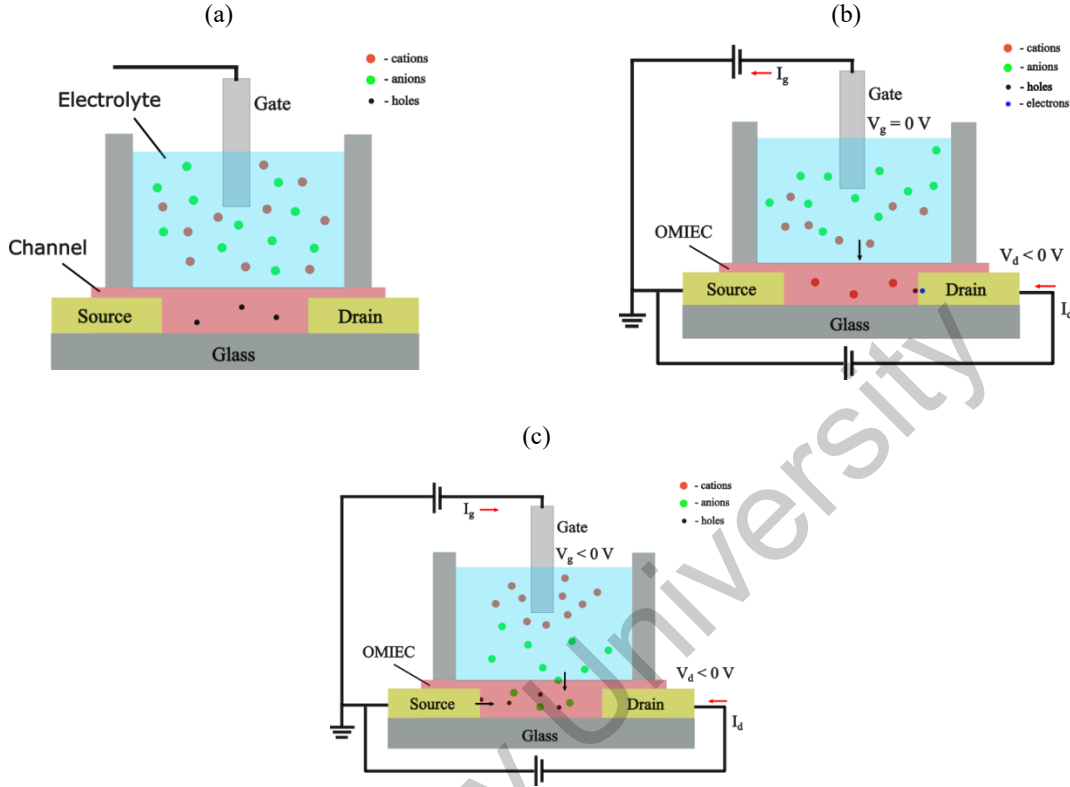


Figure 1. (a) OECT architecture, (b) electrochemical dedoping of the OMIEC channel, and (c) electrochemical doping of the OMIEC channel.

When the gate potential (V_g) is 0 V relative to the source, and the drain potential (V_d) is biased negatively relative to the source ($V_d < 0$ V), the channel potential (V_{ch}) becomes more negative compared to the gate ($\Delta V = V_g - V_{ch} > 0$ V). As a result, the potential difference ΔV between the gate and the channel creates an electrochemical driving force that pushes cations (positively charged ions) from the solution into the volume of the channel, leading to dedoping of the channel.

The electroneutrality of the channel is maintained by the removal of holes at the drain, where they recombine with electrons, leading to depletion of the channel and a reduction in its conductivity. In the case of an OMIEC channel with an initially low hole density (p_0), the dedoping process has little effect on conductivity, as it was already low. Thus, when $V_g = 0$ V and $V_d < 0$ V, the drain current (I_d) is low.

However, when the gate potential is biased more negative relative to the drain, the channel potential becomes more positive relative to the gate ($\Delta V = V_g - V_{ch} < 0$). This causes the drift-diffusion of anions into the volume of the channel (Figure 1c). The negatively charged anions are compensated by the injection of holes from the source, leading to an increase in hole density within the channel and, consequently, to a rise in its conductivity. As a result, a significant current begins to flow through the channel.

The key process that determines the conductive state of the channel in an OECT is electrochemical doping (or dedoping). Its dynamics depend on ion mobility, which is significantly lower than the mobility of electronic charge carriers. Due to the sluggishness of ions, OECTs are characterized by relatively slow switching speeds between the two steady states of the transistor. The minimum response time of an OECT is around 10 μ s [6], which is sufficient for the use of these transistors in biosensing and neuromorphic computing systems.

Since the OECT channel is in direct contact with the electrolyte, even small changes in the potentials of the gate, drain, or source significantly affect the ion dynamics in the system, resulting in noticeable changes in the drain current [9]. One of the distinguishing features of OECTs, setting them apart from other transistor types, is the ability to modulate the channel's conductivity by the drain (or source) potential. This is because the ion transport dynamics between the phases (channel/electrolyte) are controlled by the potential difference between the gate and the channel, $\Delta V = V_g - V_{ch}$, and the channel potential, in turn, depends on the drain potential [7]. Furthermore, the channel potential V_{ch} is not uniform along its length; it changes from the source potential to the drain potential. This leads to non-uniform electrochemical doping along the channel length, causing lateral ion diffusion to achieve uniform doping [8].

To demonstrate the influence of the drain potential on the steady-state characteristics of an OEET, the experimental results from our recent study are presented below [9]. Figure 2a shows IV characteristics at various fixed gate potentials for an OEET operating in accumulation mode with a p-type P3HT polymer channel. These I-V curves are referred to as the output characteristics of the transistor. As seen in Figure 2a, the output curves demonstrate asymmetry: the drain current (I_d) is significantly higher when sweeping in the direction of $V_d > 0$ V. This asymmetry in the output curves of OEETs is not always obvious. For comparison, Figure 2b presents the output characteristics of an OEET operating in depletion mode with a p-type PEDOT:PSS channel, taken from the article by D. A. Bernards and G. G. Malliaras [7]. As shown in Figure 2b, for an OEET operating in depletion mode, the output curves do not exhibit asymmetry. A more detailed discussion of the causes of asymmetry in transistor output characteristics can be found in our recent publication [9].

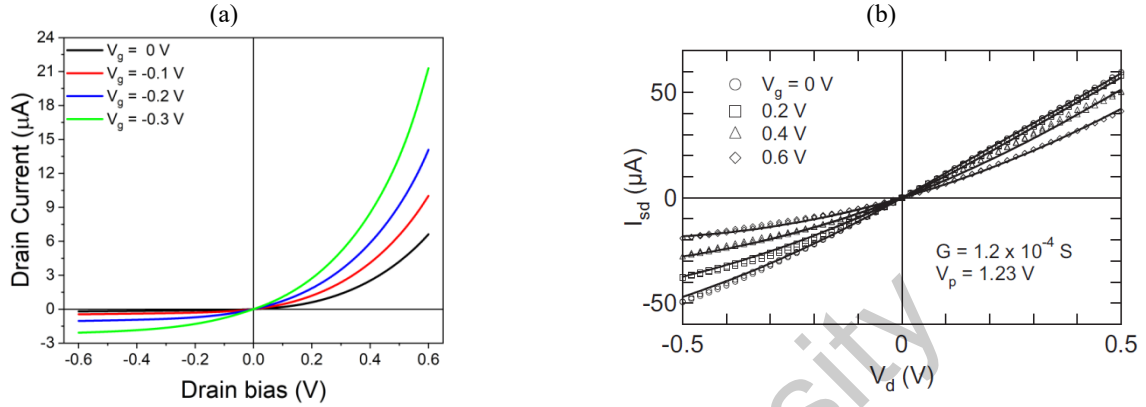


Figure 2 - Output curves of an OEET operating in accumulation mode with a P3HT channel (a) [9] and operating in depletion mode with a PEDOT:PSS channel (b) [7].

The observed asymmetry in the output curves of OEETs has important practical significance, as it allows the device to function as a rectifier (diode). The structure of the OEET can be simplified by directly connecting the gate to the source (Figure 3a). In this configuration, the OEET transforms from a three-terminal device into a two-terminal one, and the I-V curve of this device with a P3HT channel are also shown in Figure 3a. As seen from the I-V characteristics, the OEET with the gate and source short-circuited operates as a rectifier, where the drain acts as the anode and the source as the cathode.

Moreover, the rectification polarity can be easily reversed by connecting the gate directly to the drain. In this case, the source becomes the anode, and the drain becomes the cathode, as shown in Figure 3.3b. This functionality of the OEET as a rectifier with switchable polarity was first demonstrated by our group [9]. Additionally, we proposed an analytical model describing the I-V characteristics of the OEET-based rectifier and its dependence on channel geometry and material properties. This model is based on the seminal model proposed by D. A. Bernards and G. G. Malliaras for OEETs [7].

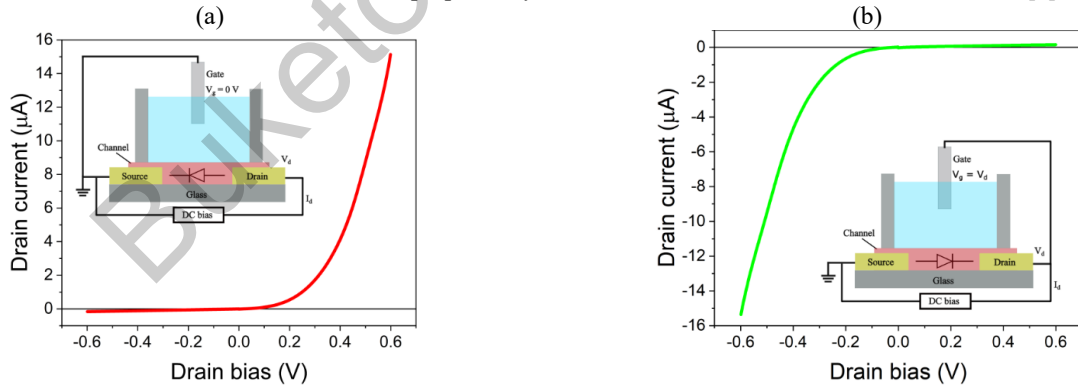


Figure 3 Organic electrochemical rectifier with switchable polarity. (a) OEET with the shorted source and gate and (b) OEET with the shorted drain and gate.

We classify the OEET with the shorted source and gate (Fig. 3a) or with the shorted drain and gate (Fig. 3b) as organic electrochemical rectifiers (OECRs). The proposed analytical model for the I-V characteristics of the OECR is presented below:

$$I = \frac{W \cdot T}{L} \cdot \mu \cdot \left[q \cdot p_0 + \frac{c_{ch}}{2} \cdot V_d \right] \cdot V_d \quad (1)$$

$$I_{нас.} = -\frac{1}{2} \cdot \frac{W \cdot T}{L} \cdot \frac{\mu \cdot q^2 \cdot p_0^2}{c_{ch}} \quad (2)$$

where W , T , and L are the parameters characterizing the geometry of the channel (width, height (thickness), and length, respectively); μ , p_0 , and c_{ch} are the parameters characterizing the physical properties of the channel (hole mobility, initial hole concentration, and specific volumetric capacitance of the channel, respectively). Equation (1) is applicable until the OECR current reaches saturation; the saturation current is defined by Equation (2).

This model allows for the analysis of the dependence of the OECR's I-V characteristics on the geometric parameters of the channel and the physical properties of the channel material. The crucial performance metric for rectifier is the rectification ratio (RR), which is defined as the ratio of the forward current (I_f) flowing through the diode when a forward voltage is applied, to the reverse current (I_r) flowing under reverse voltage ($RR = I_f/I_r$). As seen from Equation (1), geometric parameters and mobility (μ) do not affect the rectification ratio, as these parameters influence both I_f and I_r equally. However, the rectification ratio is largely dependent on the initial charge carrier density (p_0) and the specific volumetric capacitance (c_{ch}). In particular, p_0 significantly affects the ratio between I_f and I_r . Figures 4a and 4b illustrate how the I-V characteristics and RR change with different values of p_0 .

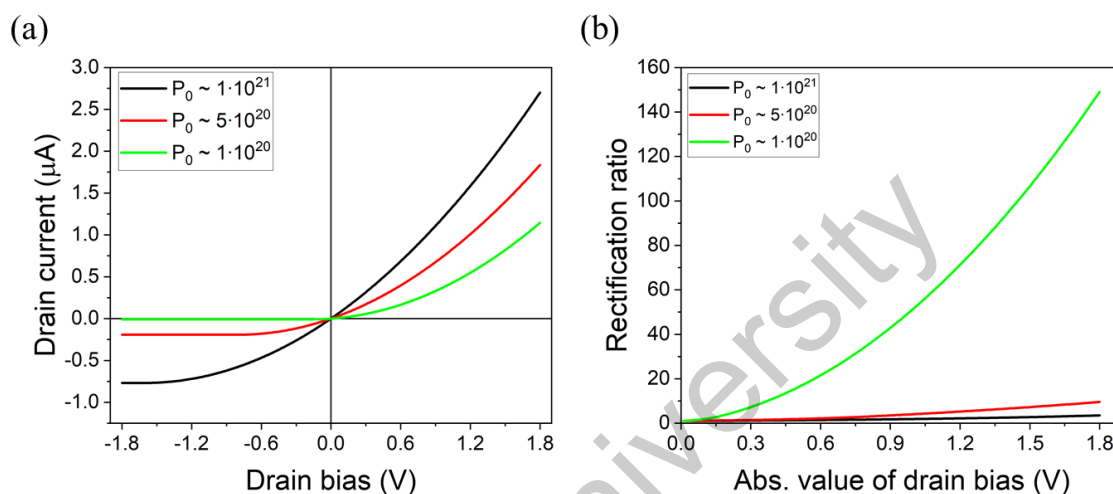


Figure 4. Dependence of the OECR I-V characteristics and rectification ratio on the initial hole concentration [9]. ($\mu = 1 \cdot 10^{-3} \text{ cm}^2 \cdot \text{V}^{-1} \cdot \text{s}^{-1}$, $c_{ch} = 1 \cdot 10^2 \text{ F} \cdot \text{cm}^{-3}$ и W, T, L : 30 nm, 100 nm and 50 μm respectively)

As shown in Fig. 4a, when a polymer with a high hole density ($\sim 1 \cdot 10^{21} \text{ cm}^{-3}$) is used as the channel, the asymmetry in the I-V characteristics is minimal. However, when p_0 is reduced by half, the asymmetry becomes more noticeable, and with a tenfold decrease in p_0 , the asymmetry becomes even more pronounced. Similarly, the rectification ratio (RR) increases as the hole concentration in the OECR channel decreases. Therefore, to develop an OECR with a high rectification ratio, OMIEC polymers with an initial charge carrier density of less than $5 \cdot 10^{21} \text{ cm}^{-3}$ should be used.

The fundamental difference between OECR and other diodes based on organic materials lies in the rectification mechanism [10]. In traditional diodes, the asymmetry in current arises due to the bending of energy bands at the interface. In OECR, the current asymmetry is caused by electrochemical doping of the channel under forward bias and dedoping under reverse bias [9]. Additionally, current asymmetry is observed in nanoporous systems [6], where it occurs due to the nonuniform geometry of the nanopores and the distribution of surface charges along their walls. However, synthesizing nanoporous films with pronounced conductivity asymmetry is a complex process that requires precise control of pore morphology. In this respect, OECR is more attractive, as it does not require creating a heterojunction or nanoporous films with a specific geometry.

At this stage of our research, we have proposed an analytical model of the OECR based on the Bernards and Malliaras model for OECTs. We have demonstrated the possibility of using OECTs as rectifiers with switchable rectification polarity. The next important stage of our research is the development of an OECR with negative differential resistance, which is crucial for designing a neuron circuit based on the OECR.

Reference

1. Tian, Z., Zhao, Z., & Yan, F. (2024). Organic electrochemical transistor in wearable bioelectronics: Profiles, applications, and integration. *Wearable Electronics*, 1, 1–25. <https://doi.org/10.1016/j.wees.2024.03.002>
2. Zhao, Z., Tian, Z., & Yan, F. (2023). Flexible organic electrochemical transistors for bioelectronics. *Cell Reports Physical Science*, 4(11), 101673. <https://doi.org/10.1016/j.xcrp.2023.101673>
3. Niu, Y., Qin, Z., Zhang, Y., Chen, C., Liu, S., & Chen, H. (2023). Expanding the potential of biosensors: a review on organic field effect transistor (OFET) and organic electrochemical transistor (OECT) biosensors. *Materials Futures*, 2(4), 042401. <https://doi.org/10.1088/2752-5724/ace3dd>
4. Paulsen, B. D., Fabiano, S., & Rivnay, J. (2021b). Mixed Ionic-Electronic transport in polymers. *Annual Review of Materials Research*, 51(1), 73–99. <https://doi.org/10.1146/annurev-matsci-080619-101319>
5. Friedlein, J. T., McLeod, R. R., & Rivnay, J. (2018b). Device physics of organic electrochemical transistors. *Organic Electronics*, 63, 398–414. <https://doi.org/10.1016/j.orgel.2018.09.010>

6. Colucci, R., De Paula Barbosa, H. F., Günther, F., Cavassin, P., & Faria, G. C. (2019). Recent advances in modeling organic electrochemical transistors. *Flexible and Printed Electronics*, 5(1), 013001. <https://doi.org/10.1088/2058-8585/ab601b>
7. Bernards, D. A., & Malliaras, G. G. (2007b). Steady-State and transient behavior of organic electrochemical transistors. *Advanced Functional Materials*, 17(17), 3538–3544. <https://doi.org/10.1002/adfm.200601239>
8. Guo, J., Chen, S. E., Giridharagopal, R., Bischak, C. G., Onorato, J. W., Yan, K., Shen, Z., Li, C., Luscombe, C. K., & Ginger, D. S. (2024). Understanding asymmetric switching times in accumulation mode organic electrochemical transistors. *Nature Materials*. <https://doi.org/10.1038/s41563-024-01875-3>
9. Ilyassov, B., Zavgorodniy, A., Alekseev, A., Aldasheva A. (2025). Rectifying behavior of organic electrochemical transistors. *Physica B: Condensed Matter*, 696, 416620 <https://doi.org/10.1016/j.physb.2024.416620>
10. Kim, Y., Kim, G., Ding, B., Jeong, D., Lee, I., Park, S., Kim, B. J., McCulloch, I., Heeney, M., & Yoon, M. (2021b). High-Current-Density organic electrochemical diodes enabled by asymmetric active layer design. *Advanced Materials*, 34(7). <https://doi.org/10.1002/adma.202107355>

УДК 669.017.16

ИССЛЕДОВАНИЕ ВЛИЯНИЕ МОЛИБДЕНА И КРЕМНИЯ НА ВЫСОКОЭНТРОПИЙНЫЙ СПЛАВ КАНТОРА

Исагулов А.З., НАО «Карагандинский технический университет имени Абылкаса Сагинова», г. Караганда, Казахстан

Квон Св.С., НАО «Карагандинский технический университет имени Абылкаса Сагинова», г. Караганда, Казахстан

Куликов В.Ю., НАО «Карагандинский технический университет имени Абылкаса Сагинова», г. Караганда, Казахстан

В работе [1] авторами предложен новый тонкоструктурный ВЭС $\text{CrFeNiAl}_{0,27}\text{Si}_{0,11}\text{Mo}_{0,22}$, полученный методом дуговой плавки. В результате проведенных экспериментальных наблюдений получены сплавы с довольно высокими механическими свойствами. Также данный сплав обладает превосходной коррозионной стойкостью за счет образования тонкой пленки оксида молибдена.

Такое значительное увеличение прочностных характеристик авторы работы связывают с образованием тонкой дуальной структуры, образованной пластинками ВСС и АСС-растворами.

Надо отметить, что данные этого исследования хорошо согласуются с результатами работы [2], где также было отмечено, что введение Мо положительно влияет на прочность при сохранении высокой пластичности. В исследовании [3] авторами разработан новый сплав FeCoCrNiMoSi_x с различным содержанием Si в соответствии с атомным соотношением $\text{Fe:Co:Cr:Ni:Mo:Si} = 1:1:1:1:1:x$ (где $x=0,5;1,0;1,5$). Авторами было установлено, что введение кремния в сплав системы FeCoCrNiMo преобразует двухфазную структуру сплава в трехфазную типа FCC + НСР + ВСС. С увеличением содержания кремния структура приобретает дендритный столбчатый характер, а при увеличении содержания Si до $x = 0,9$ и $1,0$ в сплаве образуется твердая силикатная фаза, причем при этом наблюдается четкая сегрегация элементов.

Таким образом, результаты исследований в вышеуказанных работах показали, что легирование ВЭС молибденом и кремнием приводит к значительному упрочнению, причем в ряде случаев пластичность сплавов сохраняется на прежнем уровне или даже возрастает. Надо отметить, что молибден оказывает большое влияние на прочность сплава, чем кремний.

Проведенный информационный анализ показал положительное влияние Мо и Si на прочность и пластичность сплавов системы Fe-Cr-Co-Ni-Mn. Упрочнение сплавов при сохранении или даже повышении пластичности происходит за счет образования новых фаз внедрения типа σ - и μ - фаз и фаз Лавеса, равномерно распределенных в вязкой матрице твердого раствора. Однако, все исследования касаются только «классических» ВЭС, поэтому полученные результаты невозможно просто транслировать на КВЭС, т.к. они представляют собой совершенно другие исходные фазовые системы. Не исследовались также другие свойства ВЭС, например, жидкотекучесть, которая является важной технологической характеристикой. Соответственно, исследования влияния Мо и Si на прочность, пластичность и другие свойства являются актуальной и перспективной задачей.

В лаборатории Международного центра материаловедения НАО «Карагандинский технический университет имени Абылкаса Сагинова» были проведены лабораторные испытания по выплавке опытных образцов.

В качестве шихтовых материалов использовались ферромарганец марки FeMn80C05 , феррохром марки FC005 , феррониобий марки FNb60 , никель катодный марки N1 , металлический кобальт марки K1Au и ферромolibден марки FMo60 . Химический состав компонентов шихты приведены в таблице 1. Состав шихты рассчитывался таким образом, чтобы содержание Мо составляло 5, 10, 15% масс., содержание Nb около 14% масс., остальные элементы примерно в равных долях.

Дисперсность всех компонентов на 90% была представлена фракцией 2-3 мм. Фракционный состав материалов определялся на аналитической просеивающей машине AS 200 control (Retsch, Германия). Далее